Full Articles

Mesomorphism and crystal packing of dichotomous compounds; X-ray crystal structure of *N*-(4-hexyloxybenzylidene)-*p*-toluidine*

L. G. Kuz´mina,★ P. Kalle, and A. V. Churakov

N. S. Kurnakov Institute of General and Inorganic Chemistry, Russian Academy of Sciences, 31 Leninsky prosp., 119991 Moscow, Russian Federation. Fax: +7 (495) 954 1279. E-mail: kuzmina@igic.ras.ru

The crystal structure of *N*-(4-hexyloxybenzylidene)-*p*-toluidine (**1**) was determined at 150, 273, 295, and 320 K. Compound **1** was studied by differential scanning calorimetry (DSC). According to the DSC analysis, compound **1** exhibits monotropic mesomorphism associated with Cr—Iso—N—S—Cr phase transitions. The crystal packing is built up from alternating loosely packed aliphatic and closely packed aromatic regions, which is typical of enantiotropic mesomorphic compounds. In the closely packed regions, there are two types of weak directional interactions, such as π···π stacking interactions and weak C—H O hydrogen bonds, which link the molecules into centrosymmetric dimers. The thermal behavior of compound **1** and its relation to the crystal packing are discussed.

Key words: monotropic mesomorphism, X-ray diffraction, crystal packing, 4-substituted benzylidenetoluidines.

Thermotropic mesomorphic compounds are key components of an important class of liquid-crystalline (LC) materials. A unique feature of these compounds is that they can form a mesophase on heating. A mesophase is a special aggregation state of the compound because it is both formed and decomposed through phase transitions and exhibits properties typical of both liquids (viscosity, fluidity) and crystals (anisotropy of magnetic, electrical, and optical properties), *i.e.*, it is actually a structured liquid. The first data on mesophases appeared about 130 years ago.[1] Nevertheless, potentially mesomorphic compounds continue to attract considerable attention.[2—7] Researchers still attempt to create a theory of mesophases.[8—18] However, these attempts can hardly be considered a success since none of the available theories provide adequate calculated enthalpies of phase transitions and allow the prediction of their number. This apparently implies that the models of mesophases underlying the theories do not reflect some essential structural features of mesophases.

The single-crystal X-ray diffraction (XRD) analysis provides detailed information about the structure of a crystalline phase directly preceding a mesophase. Besides, the

* Dedicated to Academician of the Russian Academy of Sciences I. L. Eremenko on the occasion of his 70th birthday.

Published in Russian in *Izvestiya Akademii Nauk. Seriya Khimicheskaya,* No. 6, pp. 1054—1060, June, 2020.

displacement parameters of atoms derived from XRD experiments allow the estimation of the relative ability of individual atomic fragments to transfer into a molten state on heating. Therefore, XRD combined with the DSC analysis can provide new information for the construction of an adequate model of a mesophase.

It is known that dichotomous compounds exhibit mesomorphism, *i.e.*, they have a molecular structure composed of at least two structurally and/or chemically contrasting portions, such as a rigid core (most often, an aromatic or unsaturated moiety) and a conformationally flexible peripheral part (most often, an aliphatic moiety). The dichotomous nature of the molecules is responsible for unusual properties of the compounds, in particular, mesomorphism, although dichotomism does not necessarily imply that the compound has mesomorphism.

Previously, we found that the crystal packings of mesomorphic compounds are built up from alternating aliphatic and aromatic regions, the aliphatic regions being very loosely packed. On the contrary, aromatic regions are characterized by a close packing stabilized by numerous dispersion interactions and secondary bonds (weak directional interactions).[19—27]

We suggest that this inhomogeneity of the crystal packing is responsible for anomalous melting of mesomorphic compounds through the intermediate formation of a mesophase. As the temperature increases, the melting first occurs in loosely packed aliphatic parts, whereas aromatic regions retain a short-order structure within a certain temperature range due to weak directional interactions. A further increase in the temperature should lead to a stepwise breaking of secondary bonds of different nature. The disruption of a large number of secondary bonds of the same type in the crystal should be accompanied by a thermal effect, *i.e.*, should occur as a phase transition. Hence, the number of phase transitions in the mesophase should depend on the number of different types of secondary bonds in the initial crystal.

Previously, we reported the evidence that the crystal melting begins in aliphatic regions with retention of structured aromatic regions, as demonstrated by X-ray diffraction analysis of *N*-(4-decyloxybenzylidene)-*p*-toluidine (**2**)[24] at different temperatures (120, 295, 320, 333 K), including the temperature close to the melting point (338 K). An increase in the temperature of the X-ray diffraction experiment was accompanied by an increase in the anisotropic displacement parameters of the terminal atoms of aliphatic chains. In the X-ray diffraction experiment at a temperature close to the melting point of the crystals, this effect is so strong that it is more correct to refine the structure using a model with disordered terminal moieties (butyl, pentyl), actually implying the random motion in these regions.

Here we report the results of the X-ray diffraction study of *N*-(4-hexyloxybenzylidene)-*p*-toluidine (**1**), which is a homolog of **2**, at 150 (**1a**), 273 (**1b**), 295 (**1c**), and 320 K (**1d**).

Results and Discussion

Calorimetry. Compound **1** was studied by simultaneous DSC analysis and polarized light microscopy of the sample on heating and cooling. It was shown that the Cr—Iso—N—S—Cr phase transitions take place in this compound. The phase transition temperatures are 58.5, 49.3, 42.9, and 35.1 °C, respectively. On heating, compound **1** undergoes a transition into an isotropic melt without formation of a mesophase. The cooling of the melt to 49.3 °C results in the formation of a nematic phase followed by the formation of a more structured smectic phase on further cooling to 42.9 °C. At 35.1 °C, compound **1** undergoes a phase transition to the crystalline phase. Therefore, compound **1** exhibits monotropic mesomorphism.

X-ray diffraction analysis. The low-temperature molecular structure of **1** is shown in Fig. 1. There are two crystallographically independent molecules with very similar geometric parameters per asymmetric unit.

Both independent molecules have a nearly planar skeleton. The twist/fold components of the dihedral angles between the benzene rings are 5.44/3.92° and 3.18/2.34° in two independent molecules. In both molecules, the alkoxy group has a planar backbone with a *trans* conformation with respect to C—C bonds. This group is nearly coplanar with the plane of the conjugated moiety of the molecule.

The crystal packing of **1** is shown in Fig. 2.

This crystal packing is schematically presented in Fig. 3. A similar schematic pattern is true for compound **2**, although the aromatic region in compound **1** differs from that in **2**.

According to this scheme, the packing consists of alternating aliphatic and aromatic regions, which is typical of the crystals of mesomorphic compounds.[19—27] An analysis of intermolecular distances in the aliphatic regions (Fig. 4) shows that all these distances are long.

Only the distances between the terminal atoms of adjacent columns are close to the sums of the corresponding van der Waals radii (~2.5 Å for H···H and ~3.9 Å for C···C).

These data provide evidence that the aliphatic regions in the crystal of **1** are loosely packed due to high conformational flexibility of the aliphatic chains during the crystal growth, resulting in an increase in their effective sizes.

As opposed to the crystals of **2**, no sharp increase in the displacement parameters of atoms of the aliphatic chains compared to atoms of the aromatic moiety was observed in the crystal structure of **1** with increasing temperature at which the X-ray diffraction data were collected, although there is a clear trend in increasing the displace-

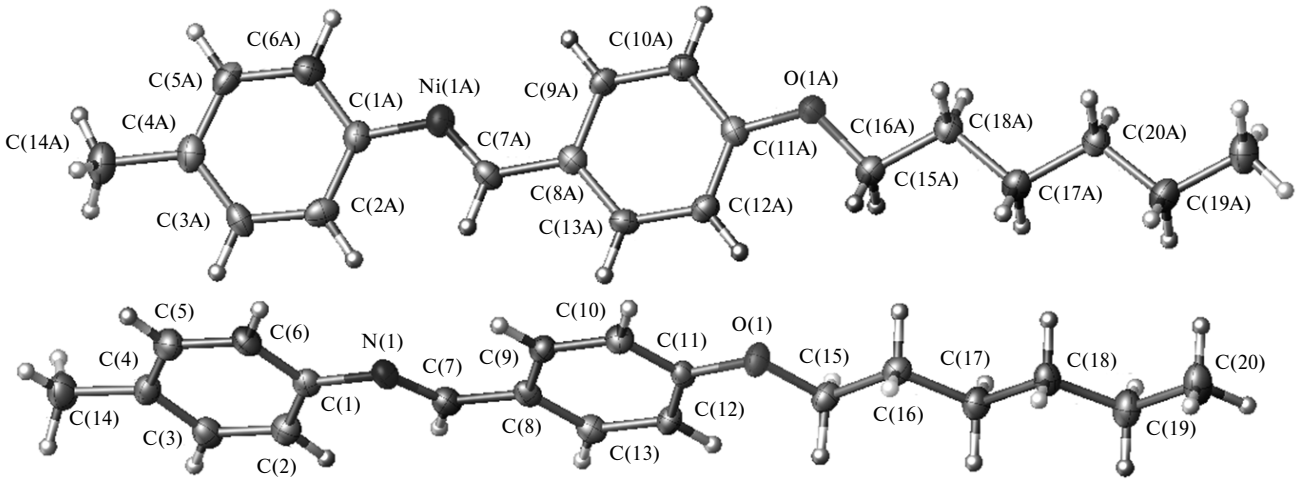

Fig. 1. Molecular structure of **1** at 150 K with anisotropic displacement ellipsoids drawn at the 50% probability level.

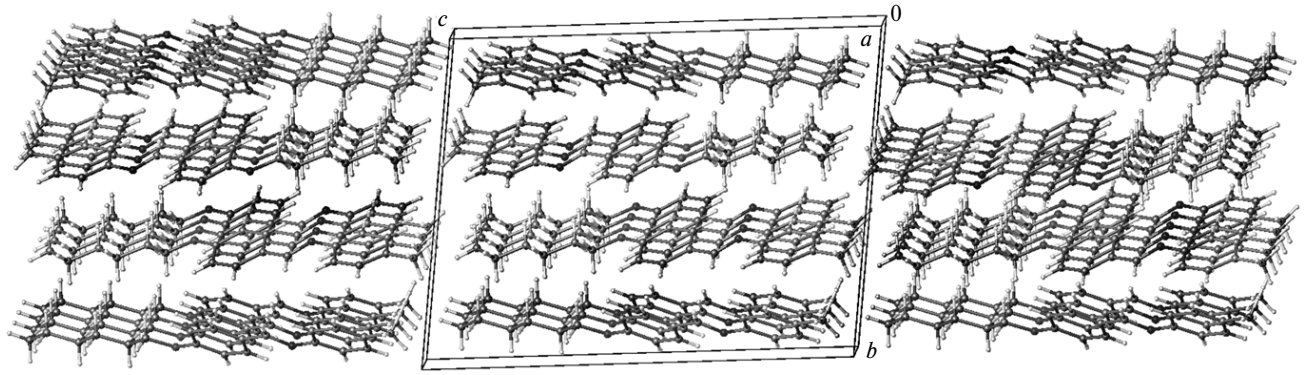

Fig. 2. Crystal packing of **1**.

ment parameters of the aliphatic atoms from the beginning to the periphery of the chain (Table 1).

This is apparently attributed to the fact that the loosely packed aliphatic regions in **1** are smaller than those in **2**, and it is these regions that are most prone to change their sizes depending on the temperature of the experiment. The unit cell parameters of compound **1** at different temperatures are given in Table 2 (see the Experimental). The changes in these parameters for **1** are at most 3.5%, whereas they reach 8% for compound **2**.

The aromatic regions in the crystal are stabilized by numerous van der Waals contacts and two types of weak directional interactions. The planar geometry of molecules **1** (like that of **2**) should facilitate the formation of π···π stacking interactions during the crystal growth. In the crystal packing of **2**, the molecules form centrosymmetric stacked dimers. As opposed to the crystals of **2**, independent molecules of only one type form stacked dimers in **1**. The mutual arrangement of the molecules in the unit cell of the crystal of **1** is shown in Fig. 5.

Crystallographically independent molecules form different substructures (Fig. 6).

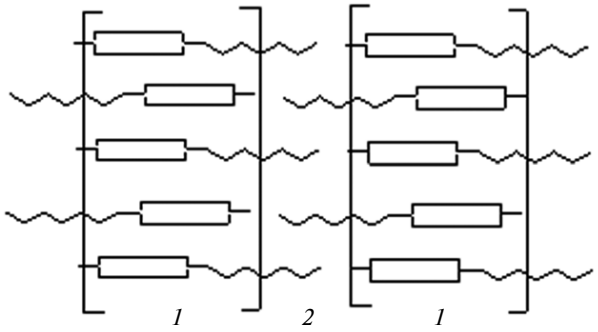

Fig. 3. Schematic representation of the crystal packing of **1**: *1*, an aromatic region, *2*, an aliphatic region.

Pairs of centrosymmetrically related molecules of one type (see Fig. 6, *a*) form a parallel dimer with a distance of 3.84 Å between the centroids of the rings characterized by efficient overlap of two π-systems. The molecules of another type (see Fig. 6, *b*) do not form such dimers. The resulting structure is a superposition of these two structures. In the crystal packing, there are also centrosym-

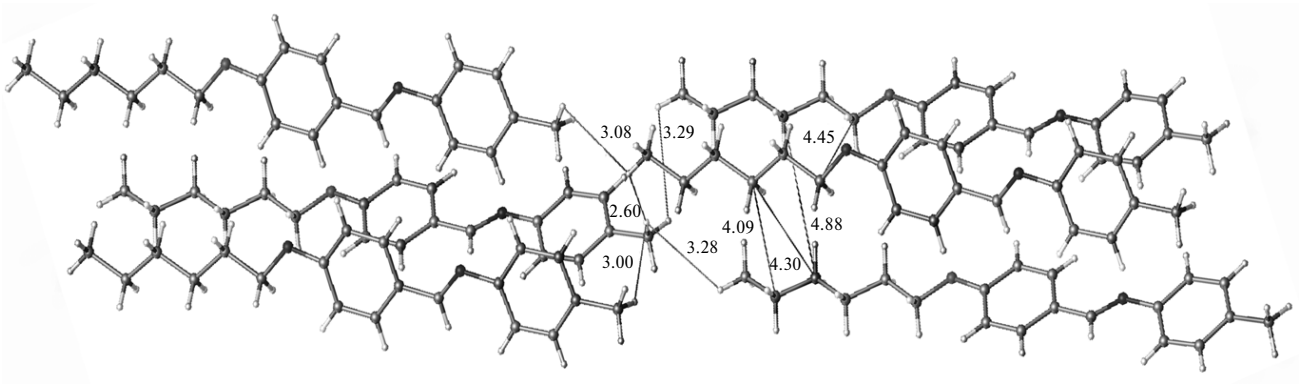

Fig. 4. Shortest intermolecular distances (Å) between atoms of adjacent aliphatic chains.

Table 1. Isotropic equivalent temperature factors B_{iso} (Å^2) of aliphatic atoms in compounds **1a—d**

Атом	1a	1b	1c	1d
O(1)	30.3	55.1	66.0	68.9
O(1A)	31.1	50.4	70.1	74.4
C(15)	28.6	50.5	64.6	67.9
C(15A)	27.9	49.9	63.9	70.2
C(16)	27.4	53.0	61.8	65.5
C(16A)	28.5	51.0	67.2	73.0
C(17)	29.8	59.1	68.6	73.3
C(17A)	31/4	55.8	73.5	84.9
C(18)	30.3	59.2	68.7	75.1
C(18A)	30.4	55.2	75.3	85.4
C(19)	38.2	74.8	87.3	99.1
C(19A)	39.7	70.1	93.1	106.2
C(20)	46.7	88.6	103.8	111.8
C(20A)	46.4	88.4	107.4	120.5

metric dimers of both independent molecules that are formed through pairs of very weak C—H···O hydrogen bonds (Fig. 7).

The hydrogen atoms H(10) and H(12A) of the independent molecules in the *ortho* positions to the electron-withdrawing alkoxy substituent are acidic, *i.e.*, they can be involved in weak hydrogen bonding with the alkoxy oxygen atoms of the neighboring molecule related to the original molecule by a center of symmetry.

Therefore, the crystal packing of compound **1** is typical of mesomorphic compounds: 1) it is composed of alternating loosely packed aliphatic and closely packed aromatic regions; 2) the aromatic regions are stabilized by two systems of weak directional interactions (π···π-stacking interactions and very weak hydrogen bonds). Nevertheless, compound **1** does not form a mesophase during melting. The only explanation of this fact is that interactions

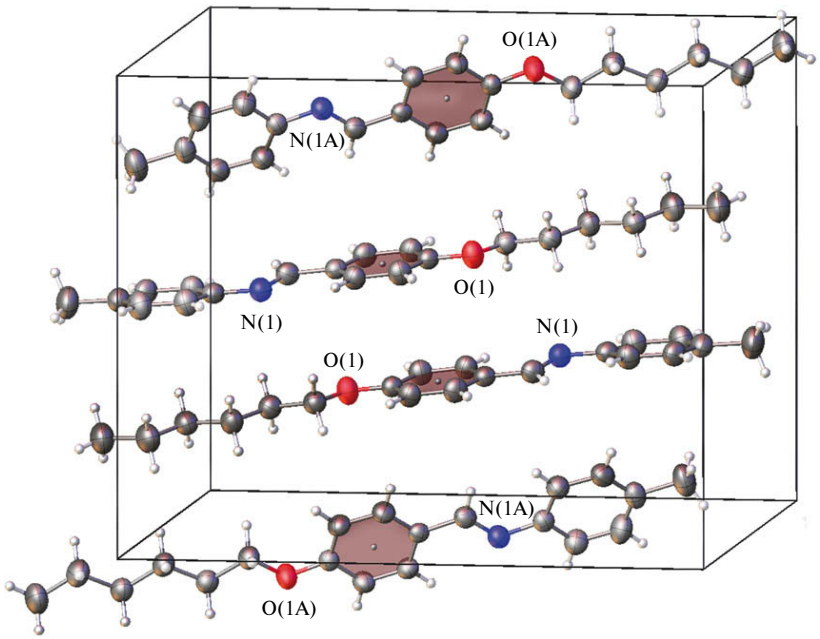

Fig. 5. Mutual arrangement of molecules **1** in the unit cell of the crystal.

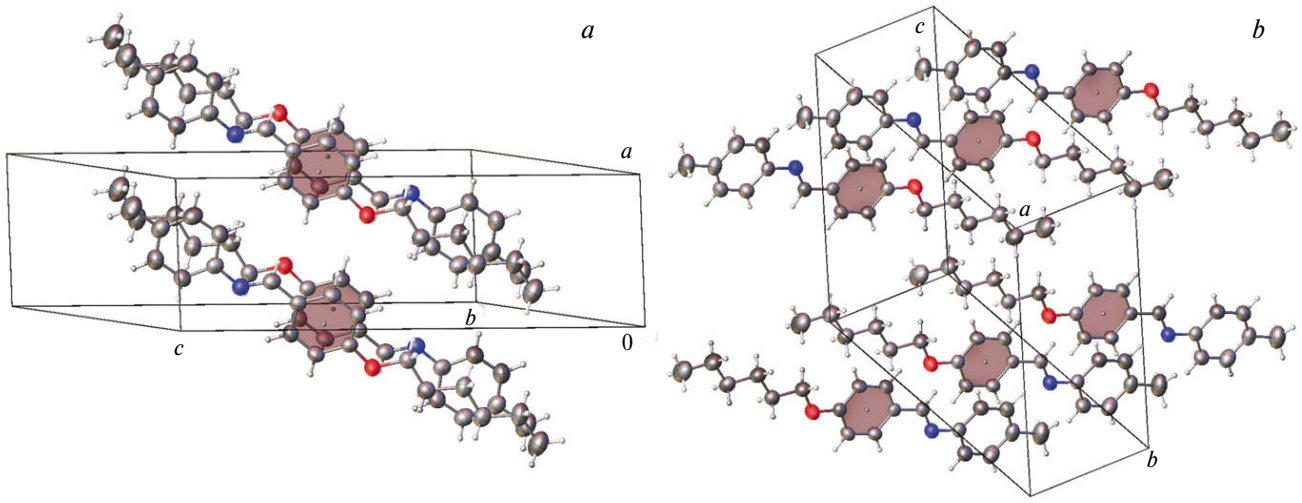

Fig. 6. Substructures formed by independent molecules.

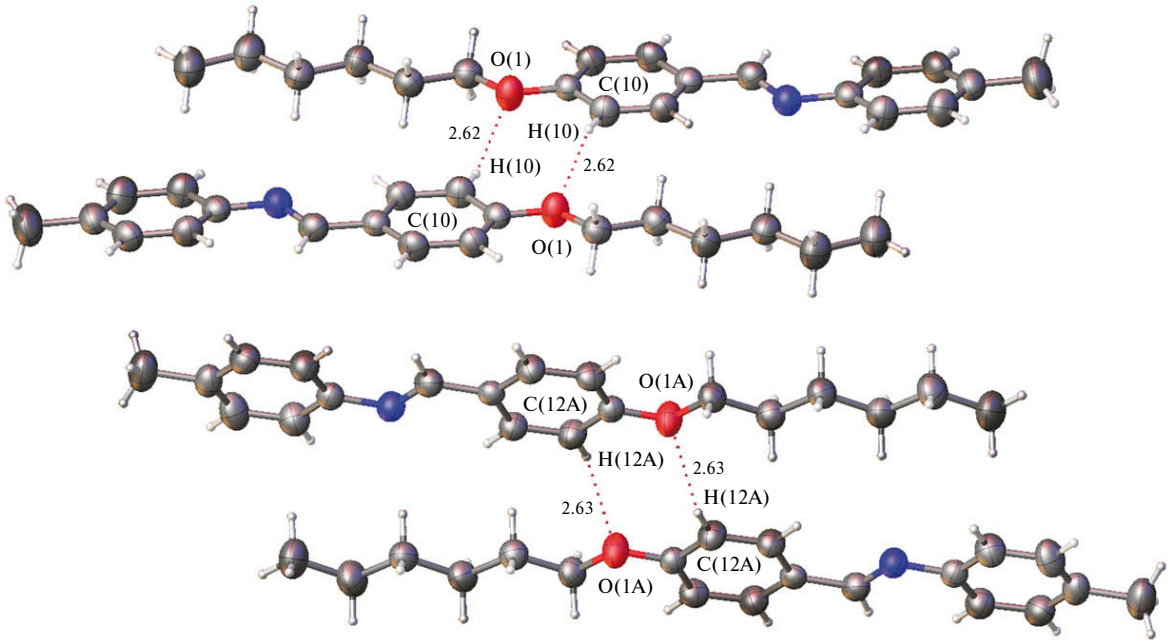

Fig. 7. Dimers formed by independent molecules *via* weak C—H···O hydrogen bonds; the distances are given in Å.

responsible for the structuring of the mesophase are also broken at a temperature close to the melting point (58.5°), but this effect is masked by the stronger melting effect. It is interesting that the cooling of the melt leads to the initial formation of a less structured mesophase followed by the formation of a more structured mesophase, *i.e.*, according to our assumption, secondary bonds begin to form (first stronger and then weaker). It is important that this process occurs in a supercooled melt, at a temperature almost 10° lower than the melting point of the initial compound. This is indirect evidence that the breaking of secondary bonds in the initial crystal occurs at a temperature lower than the melting point.

Therefore, the X-ray diffraction and calorimetric studies of compound **1** confirmed the fact that thermal motion of atoms of the aliphatic chain increases to a greater extent compared to the atoms of the rigid core with increasing temperature at which the X-ray diffraction data are collected. This is evidence that the aliphatic atoms are more prone to the transition to a liquid state, and this is responsible for nonuniform melting of these compounds. This effect is less pronounced in compound **1** compared to

compound **2**, in which the aliphatic part occupies a larger fraction of the crystalline region.

The absence of enantiotropic mesomorphism in **1** is due to the fact that weak directional interactions are broken at a temperature lower than the melting point.

Experimental

Calorimetry. A sample consisting of a small number of shapeless crystals was placed on a Linkam DSC600 Optical DSC system equipped with an Olympus BX43 polarized light microscope. The DSC analysis was performed in the heating and cooling modes at a heating rate of 5 deg min^{-1}. The thermal analysis curve of compound **1** is shown in Fig. 8.

The melting of compound **1** is not accompanied by the formation of a mesophase. The observation of the heating process using the microscope showed that most crystals melted at 58.5 °C. However, several crystals contained small inclusions (an impurity of unknown nature), which did not melt at this temperature. The melting of these inclusions was observed at 73.1 °C. The cooling of the isotropic melt was accompanied by three phase transitions at 49.3, 42.9, and 35.1 °C. The inspection using the polarized light microscope showed that the formation of the first mesophase (nematic) occurred at 49.3°. The further cooling to 42.9 °C was accompanied by the formation of a more ordered mesophase (smectic). The formation of a crystalline phase was observed at 35.1 °C. The appearance of a peak in the DSC curve measured in the cooling mode at 70.5 °C apparently corresponds to the crystallization of this impurity.

X-ray diffraction study. Single crystals suitable for X-ray diffraction were grown from a benzene—acetonitrile solvent mixture as colorless blocks belonging to the triclinic system. The crystallographic parameters and intensities of experimental reflections were measured on a SMART APEX-II CCD diffractometer at 150 (**1a**), 273 (**1b**), 295 (**1c**), and 320 K (**1d**) (ω-scanning technique, λ-Mo-*K*α radiation (λ = 0.71073 Å) for **1a,b,d** and λ-Cu-*K*α radiation (λ = 1.54178 Å) for **1c**).

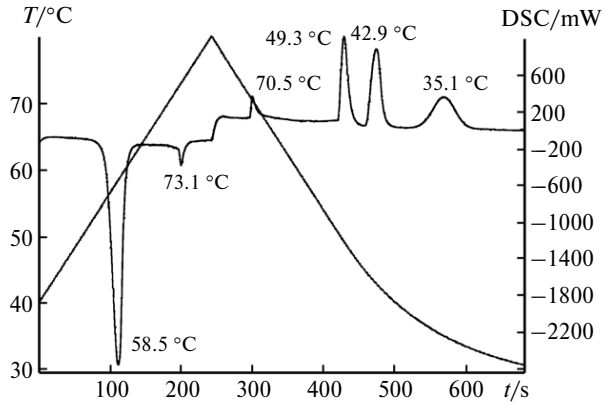

Fig. 8. DSC curve of compound **1**.

The X-ray diffraction data were processed using the SAINT program.[28]

The structures were solved by direct methods and refined by the least-squares method with anisotropic displacement parameters for nonhydrogen atoms. The hydrogen atoms were positioned geometrically and refined by the least-squares method using a riding model. All calculations were carried out using the SHELXTL-Plus program package[29] and Olex-2 software.[30] The formula of compound **1** is $C_{20}H_{25}NO$, M = 295.41. The crystals are triclinic, space group $P\bar{1}$, Z = 4. Crystallographic data at different temperatures and the structure determination and refinement statistics are summarized in Table 2.

The structural data were deposited with the Cambridge Crystallographic Data Centre (CCDC 1913119 for **1a**, 1913120 for **1b**, 1913121 for **1c**, 1913122 for **1d**). The complete X-ray structure data for the compounds are available, free of charge,

Table 2. Crystallographic data for compounds **1a—d**

Parameter	**1a**	**1b**	**1c**	**1d**
T/K	150	273	295	320
a/Å	5.9732(14)	6.0111(5)	6.0299(13)	6.061(3)
b/Å	14.785(3)	14.9645(13)	15.029(4)	15.096(6)
c/Å	19.400(4)	19.3861(16)	19.428(4)	19.368(7)
α/deg	82.368(3)	82.942(3)	83.143(18)	83.719(12)
β/deg	87.771(3)	88.393(3)	88.482(13)	88.767(14)
γ/deg	85.779(3)	85.956(3)	86.039(12)	86.026(15)
V/Å^3	1692.8(7)	1726.0(3)	1743.5(7)	1757.2(12)
d_{calc}/g cm^{-3}	1.159	1.137	1.125	1.117
Number of reflections				
measured	15003	22550	12715	13806
unique	6848	9753	4770	6192
2θ-Angle range/deg	4.76—52.7	4.23—50.39	5.94—127.99	4.23—50.44
Number of variables	401	401	401	401
GOOF по F^2	1.020	1.060	1.050	1.056
R_1/wR_2 ($I > 2\sigma(I)$)	0.0544/0.1339	0.0660/0.1322	0.0592/0.1127	0.0888/0.2499
R_1/wR_2 (all reflections)	0.1024/0.1573	0.1192/0.1527	0.1414/0.1773	0.1613/0.2799
Residual electron density (ρ_{max}/ρ_{min})/e Å^{-3}	0.24/−0.28	0.21/−0.14	0.17/−0.20	0.33/−0.19

at deposit@ccdc.cam.ac.uk or http://www.ccdc.cam.ac.uk/data_request/cif.

The X-ray diffraction study was performed using equipment of the Shared Facility Center of the N. S. Kurnakov Institute of General and Inorganic Chemistry, Russian Academy of Sciences. The commercial powdered sample for investigation was supplied by N. S. Kucherepa.

This work was financially supported by the Russian Science Foundation (Project No. 16-13-10273).

References

1. O. Lehman, *Z. Phys. Chem.*, 1889, **4**, 462.
2. A. Skoulios, D. Guillon, *Mol. Cryst. Liq. Cryst.*, 1988, **165**, 317.
3. C. Tschierske, *J. Mater. Chem.*, 1998, **8**, 1485.
4. B. Donnio, S. Buathong, I. Bury, D. Guillon, *Chem. Soc. Rev.*, 2007, **36**, 1495.
5. D. W. Bruce, P. Metrangolo, F. Meyer, C. Präsang, G. Resnati, G. Terraneo, A. C. Whitwood, *New J. Chem.*, 2008, **32**, 477.
6. F. Vera, J. L. Serrano, T. Sierra, *Chem. Soc. Rev.*, 2009, **38**, 781.
7. O. E. Piro, G. A. Echeverria, F. D. Cukiernik, *Crystallogr. Rev.*, 2017, 1.
8. W. Maier, A. Saupe, *Z. Naturforsch.*, 1960, **15a**, 287.
9. R. L. Humphrie, P. G. Jame, G. R. Luckhurs, *J. Chem. Soc. Faraday Trans. II*, 1972, **68**, 1031.
10. P. G. De Gennes, *Mol. Cryst. Liq. Cryst.*, 1973, **21**, 49.
11. W. L. Mc Millan, *Phys. Rev. A*, 1973, **8**, 1921.
12. A. Wulf, *Phys. Rev. A*, 1975, **11**, 365.
13. M. A. Cotter, *Mol. Cryst. Liq. Cryst.*, 1983, **97**, 29.
14. M. A. Osipov, *Molecular Theories of Liquid Crystals. Sections 2, Ch. III, V. 1*, Handbook of Liquid Crystals, Eds D. Demus, J. Goodby, G. W. Gray, H.-W. Spies, V. Vill, Weinheim, Wiley—VCH, 1998, p. 40.
15. G. Vertoge, W. H. Jeu, *Thermotropic Liquid Crystals*, *Fundamentals*, Berlin, Springer—Verlag, 1988, 324 pp.
16. P. G. de Gennes, J. Prost, *The Physics of Liquid Crystals*, New York, Oxford University Press, 1995, 616 p.
17. S. Singh, *Phys. Rep.*, 2000, **324**, 2—4, 107.
18. A. A. Stupnikov, M. A. Shcherbina, S. N. Chvalun, *Russ. Chem. Bull.*, 2018, **67**, 1547.
19. A. N. Kochetov, L. G. Kuz´mina, A. V. Churakov, N. S. Rukk, S. M. Pestov, *Crystallogr. Repts*, 2006, **51**, 53.
20. L. G. Kuz´mina, S. M. Pestov, A. N. Kochetov, A. V. Churakov, E. Kh. Lermontova, *Crystallogr. Repts*, 2010, **55**, 786.
21. L. G. Kuz´mina, N. S. Kucherepa, *Crystallogr. Repts*, 2011, **56**, 242.
22. L. G. Kuz´mina, N. S. Kucherepa, A. V. Churakov, *Crystallogr. Repts*, 2012, **56**, 213.
23. L. G. Kuz´mina, I. I. Konstantinov, E. K. Lermontova, *Mol. Cryst. Liq. Cryst.*, 2014, **588**, 1.
24. L. G. Kuz´mina, M. A. Navasardyan, A. V. Churakov, J. A. K. Howard, *Mol. Cryst. Liq. Cryst.*, 2016, **638**, 60.
25. L. G. Kuz´mina, I. I. Konstantinov, A. V. Churakov, *Mol. Cryst. Liq. Cryst.*, 2018, **664**, 95.
26. L. G. Kuz´mina, I. I. Konstantinov, S. I. Bezzubov, *High Energy Chem.*, 2016, **50**, 453.
27. L. G. Kuz´mina, I. I. Konstantinov, A. V. Churakov, M. A. Navasardyan, *Acta Cryst.*, 2017, **E73**, 1052.
28. *SAINT, Version 6.02A*, Bruker AXS: Madison, W1, 2001.
29. *SHELXTL-Plus*, *Version 5.10*, Bruker AXS, Madison, W1, 2001.
30. O. V. Dolomanov, L. J. Bourhis, R. J. Gildea, J. A. K. Howard, H. Pushman, *J. Appl. Crystallogr.*, 2009, **42**, 339.

Received November 11, 2019;
in revised form December 4, 2019;
accepted December 5, 2019